Biochemistry 1985, 24, 4315–4325

NMR Studies of Ion Binding to *Escherichia coli* $tRNA^{Phe}$[†]

Eva I. Hyde[‡] and Brian R. Reid*

Department of Chemistry, University of Washington, Seattle, Washington 98195

Received October 12, 1984

ABSTRACT: The effects of magnesium, spermine, and temperature on the conformation of *Escherichia coli* $tRNA^{Phe}$ have been examined by proton and phosphorus nuclear magnetic resonance spectroscopy. In the low-field proton NMR spectra we have characterized two slowly interconverting conformations of this tRNA at low magnesium ion concentrations. The relative proportion of the conformers is ion dependent but not ion specific. Magnesium affects protons in all the stems of tRNA while spermine effects are localized near the s^4U-8–A-14 and G-15–C-48 tertiary bonds. The effects seen in the proton NMR spectra are compared and correlated with those observed in the phosphorus spectra to give assignments of some of the resolved signals from the phosphate groups. The phosphorus spectra are compared with those of yeast $tRNA^{Phe}$ [Gorenstein, D. G., Goldfield, E. M., Chen, R., Kovar, K., & Luxon, B. A. (1981) *Biochemistry 20*, 2141; Salemink, P. J. M., Reijerse, E. J., Mollevanger, L., & Hilbers, C. W. (1981) *Eur. J. Biochem. 115*, 635], and the ion effects are discussed with reference to the magnesium and spermine sites found in the crystal structures of yeast $tRNA^{Phe}$ [Holbrook, S. R., Sussman, J. L., Warrant, R. W., Church, G. M., & Kim, S.-H. (1977) *Nucleic Acids Res. 4*, 2811; Quigley, G. J., Teeter, M. M., & Rich, A. (1978) *Proc. Natl. Acad. Sci. U.S.A. 75*, 64; Jack, A., Ladner, J. E., Rhodes, D., Brown, R. S., & Klug, A. (1977) *J. Mol. Biol. 111*, 315].

Spermine and magnesium have been shown to affect many of the biological functions of tRNA,[1] for example, the rate and accuracy of aminoacylation (Lovgren et al., 1978; Loftfield et al., 1981) and of translation on the ribosomes (Thompson et al., 1981). While some of these effects may be on the proteins or ribosome, some are likely to be on the tRNA structure. Although ion binding to tRNA has been studied for many years, the number and nature of the cation binding sites on tRNA and their effects on its conformation remain controversial [for reviews, see Schimmel & Redfield (1980) and Crothers & Cole (1978)]. Nuclear magnetic resonance (NMR) spectroscopy is an ideal technique for monitoring changes in molecular conformation that may accompany ion binding as the shift of each observed nucleus is dependent on its chemical environment. We have therefore used ^{1}H and ^{31}P NMR spectroscopy to examine the effects of magnesium and spermine on *Escherichia coli* $tRNA^{Phe}$. In particular, we have looked for ion-specific effects on this tRNA under conditions in which the tertiary hydrogen bonds, and, hence, the tertiary structure, are present. We have also studied the effect of temperature at different magnesium concentrations to see whether magnesium ion causes stabilization of a single structure with respect to temperature or whether it causes structural changes within the molecule.

The low-field ^{1}H NMR spectra of tRNAs contain the resonances of the hydrogen-bonded imino protons of the helical stems and of the tertiary base pairs [for a review, see Reid (1981)]. Each hydrogen-bonded imino proton gives a separate signal, the resonance position of which is mainly influenced by the ring-current effects of the neighboring base pairs. The imino proton spectrum is thus very sensitive to the orientation and distances of the neighboring rings (Arter & Schmidt, 1976). Phosphorus NMR spectra of tRNA give information that is complementary to the ^{1}H NMR spectra. From molecular orbital calculations and studies on model systems, it has been proposed that ^{31}P chemical shifts of phosphate esters depend on their bond and torsion angles (Gorenstein, 1975; Gorenstein & Kar, 1975, 1977). In the ^{31}P NMR spectra of tRNAs, most of the phosphates resonate at similar frequencies near −0.5 ppm; however, there are about 16 resolved signals on either side of this cluster (Gueron & Shulman, 1975; Salemink et al., 1979; Gorenstein & Luxon, 1979). Since all the signals coalesce on heat denaturation of the tRNA, the spread of signals must be due to the tertiary structure of tRNA. The resolved signals are therefore thought to be from phosphate groups in the loops and turns of the tRNA. By combining proton NMR studies on the hydrogen-bonded imino protons with phosphorus NMR studies of the resolved phosphate peaks, both the helical stems and the loops of the tRNA molecule are monitored.

The imino spectrum of *E. coli* $tRNA^{Phe}$ has been largely assigned from sequential nuclear Overhauser effects (Hyde & Reid, 1985). Hence, for these resonances the effects of ions can be directly related to the tRNA sequence and structure. ^{31}P NMR spectra of *E. coli* $tRNA^{Phe}$ have not previously been studied; however, since ^{31}P shifts of phosphate esters depend mainly on their conformation, the ^{31}P NMR spectra of different tRNAs are similar and can be directly compared (Gorenstein & Goldfield, 1982). The assignment of ^{31}P spectra of tRNAs remains tentative apart from the resonance at about 3.1 ppm, which titrates as a primary phosphate and is assigned

---

[†] This work was supported by research grants from the National Science Foundation (PCM8215812) and the National Institutes of Health (GM 28764). The WM500 spectrometer is supported by instrumentation grants from the Murdock Foundation, the National Science Foundation (PCM80-18053), and the National Institutes of Health (GM28764-0151).

[‡] Present address: Department of Microbiology and Immunology, University of Washington, Seattle, WA 98195.

[1] Abbreviations: D, dihydrouridine; DSS, 4,4-dimethyl-4-silapentane-1-sulfonate; EDTA, ethylenediaminetetraacetic acid; FID, free-induction decay; m^7G, 7-methylguanosine; ^{1}H, proton; NOE, nuclear Overhauser effect; NMR, nuclear magnetic resonance; ^{31}P, phosphorus-31; ppm, parts per million; s^4U, 4-thiouridine; T, ribothymidine; tRNA, transfer ribonucleic acid; Ψ, pseudouridine.

0006-2960/85/0424-4315$01.50/0

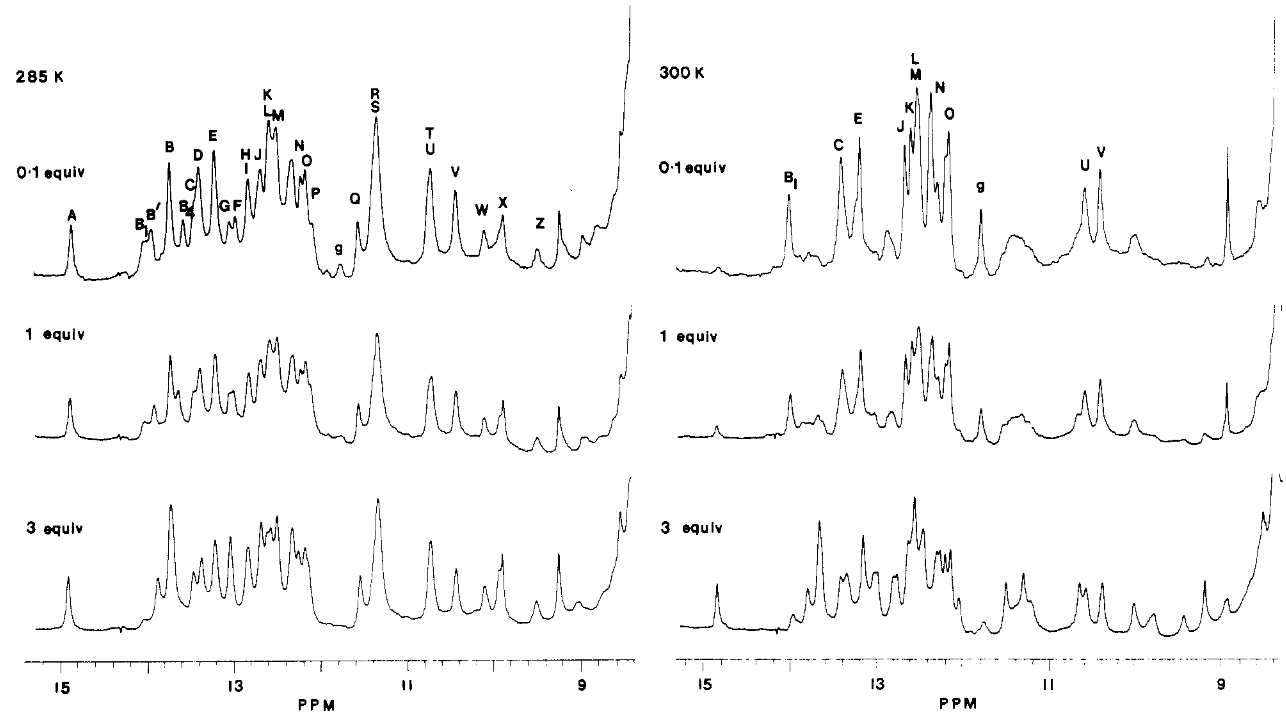

FIGURE 1: Low-field ^{1}H NMR spectrum of *E. coli* tRNA^{Phe} in 10 mM cacodylate–100 mM NaCl buffer, pH 7.0, containing (a) 0.1 equiv of magnesium, (b) 1 equiv of magnesium, or (c) 3 equiv of magnesium at 12 (left) and 27 °C (right).

to the 5′-terminal phosphate (Gueron & Shulman, 1975). Some additional assignments of the ^{31}P NMR spectra of yeast tRNA^{Phe} have been made on the basis of chemical or enzymatic modification (Salemink et al., 1979), thermal unfolding (Salemink et al., 1981), and comparison of the effects of magnesium or manganese addition with the ion binding sites seen in the crystal structure (Gorenstein et al., 1981). The assignment of three resonances to the anticodon loop is fairly firm, but that of the other resonances is more tentative. In this study we have correlated the changes observed in the ^{1}H NMR spectra of *E. coli* tRNA^{Phe} on addition of magnesium and spermine, or on heating, with those in the ^{31}P NMR spectra to obtain some phosphorus assignments. This has led to confirmation of some previous assignments and to the assignment of some peaks not previously assigned. The phosphorus spectra are compared with those of yeast tRNA^{Phe}, and the ion effects are discussed with reference to the yeast tRNA^{Phe} crystal structure.

MATERIALS AND METHODS

E. coli tRNA^{Phe} was purified as previously described by chromatography on benzoylated DEAE-cellulose (Gillam et al., 1967) followed by DEAE-Sephadex chromatography (Nishimura, 1971). Magnesium was removed from the NMR samples by dissolving the tRNA in 10 mL of 10 mM EDTA at pH 7.0 and heating to 60 °C for 5 min. The solution was immediately vacuum dialyzed against 2 L of 10 mM cacodylate, 100 mM NaCl, and 1 mM EDTA, pH 7.5, to a volume of 0.25 or 0.5 mL. It was then freeze-dried and taken up in the same volume of distilled water, and additional buffer solution was added as required. The amount of magnesium remaining after this treatment was measured on an inductively coupled plasma spectrometer and found to be 0.1 magnesium ion per tRNA.

For the ^{1}H NMR studies, 7–10-mg tRNA samples were used in 0.3 mL of buffered H_2O solution. The spectra were collected on a Bruker WM500 FT NMR spectrometer using a modified 21412 Redfield pulse as previously reported (preceding paper). Typically, 1000 scans were collected. For the ^{31}P studies, 30-mg tRNA samples in 2.5 mL of buffered D_2O solution were used. The spectra were collected on a wide-bore Bruker CXP 200 FT NMR spectrometer. Pulses of 80° were used with a sweep width of 6024 and collected into 8K data points. Gated broad-band decoupling of 1 W and a relaxation delay of 2.5 s between pulses were used to prevent excessive heating of the solution by the decoupler. Typically, 6000 scans were collected. Shifts are referenced to 85% phosphoric acid at the same temperature. Magnesium or spermine was added as small aliquots of a concentrated stock solution in the same buffer as the tRNA solution.

Transfer of saturation experiments were carried out by irradiating one peak for 0.6–1.0 s before the observation pulse. Sets of 16 scans with the decoupler on- and off-resonance were collected separately and subsequently subtracted. To determine the lifetime of each conformer, two types of experiment were performed. In the first experiment, both the rate of transfer of saturation and the steady-state effect were measured by irradiating one peak for varying times before observing the height of the related peak. In the second experiment, the apparent spin-relaxation time τ_{1A} of this related peak was measured directly by saturation–recovery. The acceptor peak was irradiated for 0.3 s, and its height was measured as a function of the delay time before the observation pulse. In both the transfer of saturation and the saturation–recovery experiments, the slope of a graph of ln $(M_\infty - M_t)$ vs. time is $1/\tau_{1A}$, where M_t is the intensity of the peak at time t. The steady-state transfer of saturation effect $M_\infty/M_0 = \tau_{1A}/T_{1A}$, where T_{1A} is the spin–relaxation time. The lifetime is then obtained from the relationship (Forsen & Hoffman, 1963)

$$\frac{1}{\tau_A} = \frac{1}{T_1A} + \frac{1}{\tau_1A}$$

RESULTS AND DISCUSSION

Low Ion Concentrations. Figure 1 shows the imino region of the proton NMR spectra of *E. coli* tRNA^{Phe} in the presence of low magnesium concentrations at 12 and 27 °C. At these low magnesium concentrations, the tRNA structure is destabilized and flexible, and the imino protons alternate between the hydrogen-bonded form and an open state in which they are in fast exchange with solvent. This exchange causes the hydrogen-bonded imino proton resonances to lose intensity and broaden with increasing temperature (spectroscopic melting). At the lowest concentration of magnesium, it appears that some melting occurs even at 12 °C. The ^{31}P spectrum under these conditions shows only a few resolved peaks, some of which are of partial intensity showing that the tRNA has lost some of its native structure.

In the ^1H NMR spectrum, at 0.1 equiv of magnesium, peak B is split into four peaks, named B_1, B′, B, and B_4. In addition to this splitting, a small peak is seen at 11.79 ppm, peak g. As the magnesium concentration increases peaks, B_1 and g decrease in intensity and B_4 shifts into B. Conversely, as the temperature is increased at constant magnesium, B_1 and g increase in intensity. Similar behavior of the peaks is observed upon addition of sodium ions instead of magnesium ions, but more than 0.5 M sodium is needed to obtain full intensity in peak B_4, and the shift of this peak is unaffected by sodium (data not shown).

Figure 2b–e shows the difference spectra obtained in the presence of minimal magnesium at 12 °C when peaks B_1, B_4, g, and G are selectively irradiated. Irradiation of B_1 causes a large decrease in intensity of peak B_4 and vice versa. The effect from B_1 to B_4 is larger than the effect on the large intervening peak B, showing that the effects are not due to nonselective irradiation. Irradiation of the small partial peak g similarly causes a large decrease in peak G and vice versa. These irradiation effects are too large to be due to nuclear Overhauser effects between the imino protons of adjacent base pairs. NOEs occur between nuclei that are close in space when saturation of one nucleus affects the intensity of the resonance of its neighbor, depending on the inverse sixth power of their distance (Noggle & Shirmer, 1971). NOEs between imino protons of neighboring base pairs are typically less than 5% in size. A typical nearest neighbor NOE between G (CG-13) and A (s^4U-8–A-14) can be seen in Figure 2e. Apart from size considerations, the irradiation effects are unlikely to be NOEs as both B_1 and B_4 are AU base pairs [shown by their chemical shifts and their NOEs to sharp aromatic adenine C2-H resonances (Sanchez et al., 1980)] and there are no adjacent AU base pairs in this tRNA. The irradiation effect must therefore be due to transfer of saturation. Transfer of saturation occurs if a nucleus exists in two chemical environments, with different chemical shifts, which are in slow exchange on the NMR time scale. If the resonance from one conformation is saturated and the nucleus exchanges into the other environment before relaxing, there is a decrease in intensity of the resonance associated with the second environment (Forsen & Hoffman, 1963). B_1 and B_4 are therefore the two partial resonances of a single imino proton in two different chemical environments, as are peaks g and G. *E. coli* tRNA^{Phe} must therefore exist as a mixture of two conformers in slow exchange under these conditions. From Figure 1, the intensity of each peak, and hence the amount of each conformer, is dependent on the ion concentration and temperature. This suggests that the difference between the conformers is in the number of bound ions; dissociation of ions being favored at higher temperatures. However, the ratio of the two conformers is not magnesium specific as addition of sodium also affects the proportion of each.

The identity of peak G is revealed by the NOE between G and A (Figure 2e). This NOE is consistent with the effects observed at higher magnesium concentrations, and because A is from the s^4U-8–A-14 imino proton, G has been firmly assigned to the CG-13 imino proton (preceding paper). At higher magnesium concentrations B_4 merges with B; peak BB_4 gives an NOE to G, and peak G gives an NOE to BB_4 as well as to peak A. At high sodium concentrations, when F and G merge but B_4 is still separated from B, the double peak FG gives NOEs to peak A and to peak B_4 but not to peak B, and conversely, B_4 gives an NOE to FG. Hence, peak B_4 must be the other neighbor of CG-13, namely, AU-12. B_1 and g therefore correspond to the low-salt alternate conformation of UA-12 and CG-13, respectively. Peak A (s^4U-8–A-14) is not split, and although the 14–12 ppm region of the spectrum is crowded and may hide splittings, no transfer of saturation effects have been observed for other peaks. Thus, the main observable difference between the two conformers is in base pairs 12 and 13 in the D stem of tRNA. The largest difference in the imino proton shift between the conformers is for base pair 13, peaks G and g, which in the low-salt conformer is shifted upfield almost into the region of the spectrum where

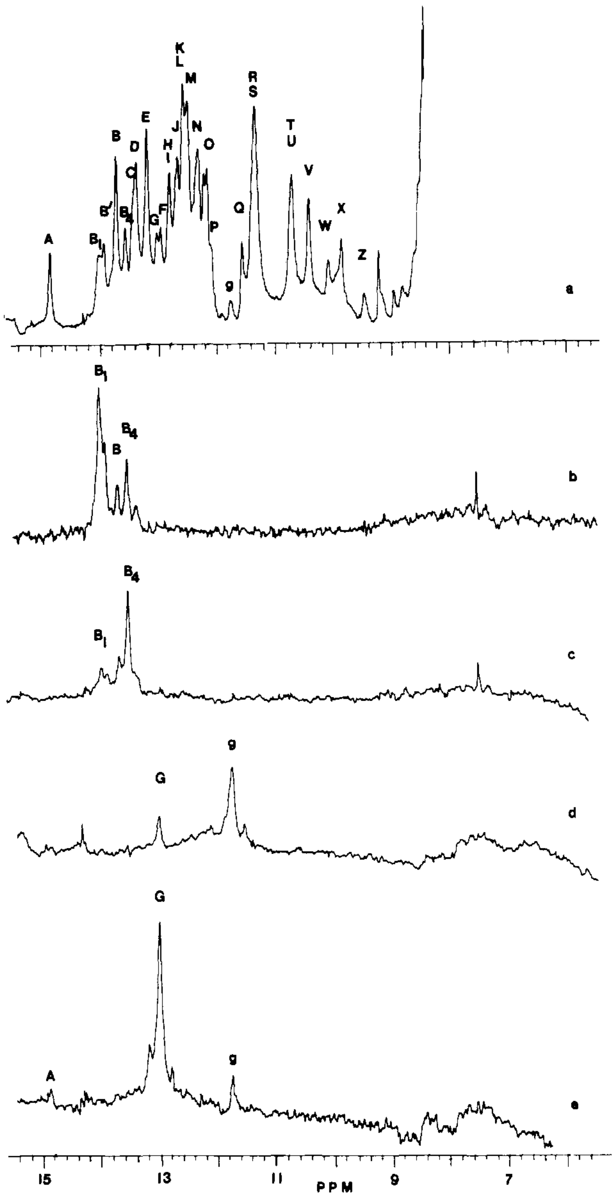

FIGURE 2: (a) Low-field ^1H NMR spectrum of *E. coli* tRNA^{Phe} in 10 mM cacodylate–100 mM NaCl buffer, pH 7.0, containing less than 0.1 equiv of magnesium at 12 °C. (b–e) Difference spectra obtained on irradiation of (b) B_1 for 0.6 s, (c) B_4 for 0.6 s, (d) g for 0.6 s, and (e) G for 1.0 s.

non-hydrogen-bonded imino protons might be expected to resonate. Peak g is in slow exchange with the solvent in this conformer and so must still be inaccessible to water. The imino proton of base pair 12 resonates 0.4 ppm further downfield in this alternate conformation than in the native one. This may be due to less stacking with the neighboring base pair 13. The conformational effect may be a partial twisting or opening of base pair 13 at low ionic strengths. The tertiary base pairs appear to be unaffected by this conformational change. Further interpretation of the chemical shift data in structural terms is not possible (see paragraph at end of paper regarding supplementary material).

For peaks in slow exchange, the apparent spin-relaxation rate is the sum of the intrinsic rate and the exchange rate. The steady-state transfer of saturation effect is the apparent relaxation rate divided by the intrinsic rate. Hence, the lifetime of each conformation can be calculated from the size of the steady-state transfer of saturation effect and the relaxation time of the affected proton (Forsen & Hoffman, 1963). For peaks B_4 and G, which belong to the predominant conformer, it is possible to measure relaxation times by selective saturation recovery experiments as the effect of saturation of B_4 or G on the coupled peaks B_1 and g is small (~8%). Because irradiation of B_1 causes a larger effect on B_4 (16%), selective saturation of B_1 is not possible, and saturation-recovery experiments on B_1 would measure the coupled relaxation of B_1 and B_4. The apparent relaxation rate of B_1, the low-salt conformer, was therefore determined from the time dependence of the transfer of saturation from B_4. This method is less accurate than the saturation recovery method as it takes a finite time to saturate B_4 compared to the rate of the transfer of saturation to B_1. The apparent relaxation rate of B_4 was measured again by this method to compare the two methods. From saturation-recovery experiments, the relaxation time of B_4 was 12 s^{-1} while transfer of saturation experiments gave 12.4 s^{-1}, in good agreement. From the relaxation times and the steady-state transfer of saturation effects in 10 mM cacodylate-100 mM NaCl buffer, pH 7.5, at 12 °C, the lifetimes of the peaks B_4 and G (i.e., the high-salt conformer) were both 0.6 s while that of peak B_1 (from the low-salt conformer) was 1.7 s. The lifetimes of the conformers indicate an equilibrium constant between them of about 3 in favor of the high-salt form under these conditions. This is consistent with the relative intensities of peaks G and g.

Effect of Magnesium. At magnesium concentrations above 5 equiv, there is no peak splitting in the ^{1}H NMR studies. The effect of magnesium on the shifts of the imino protons at 17 °C is shown in Figure 3. Most of the peaks shift slightly with magnesium. The largest shift changes are experienced by peaks B′, D, L′, and U, which move upfield, and by B_4, F, and N′, which move downfield. The effects start to occur simultaneously at the lowest magnesium concentration except for L′, which only shifts above 3 mM magnesium, after B_4. L′ is therefore affected by a weaker magnesium binding site than is B_4. The shift changes for these peaks reach completion at different magnesium concentrations, indicating that different binding processes are being monitored. Effects are seen in all the stems, but each effect is a very local one, even protons in the same base show different magnesium effects. For example, in the T stem peak U, from Ψ-55 N1-H, has a continuous upfield shift with magnesium; however, peak Q, from the Ψ-55-N3-H proton, shows a shift only up to 5 mM magnesium, and Z, the G-18- Ψ-55 tertiary hydrogen bond, shows no change in shift with magnesium. One set of shifts that may be correlated are those of W, assigned to the imino proton of guanine-63, which shifts 0.1 ppm upfield while H, assigned to GC-53, shifts 0.1 ppm downfield over a similar magnesium range. These effects could be due to changes in the position of the intervening base pair GC-52, which resonates in the multiple peak N. One of the components of peak N does shift over this range of magnesium concentrations, but its specific identity cannot be established.

^{31}P NMR spectra as a function of magnesium concentration at 27 °C are shown in Figure 4. The ^{31}P spectra were taken at 0.34 mM tRNA rather than the 1 mM concentration used for the ^{1}H NMR studies; hence, the number of equivalents of magnesium is 3 times higher than that for the same magnesium concentration in the ^{1}H NMR spectra. Since the binding constants of the ions are higher than the concentrations of tRNA used in the NMR studies (Schreier & Schimmel, 1974, 1975; Stein & Crothers, 1976a,b), binding should be stoichiometric, and it is the number of equivalents of ions that is important in comparing ion effects between spectra.

As in the ^{1}H NMR spectra, several of the ^{31}P peaks shift with magnesium. Peak A, from the 5′-terminal phosphate group, is extremely sensitive to pH variation in this pH region and so may be reflecting slight pH changes rather than ion-induced changes and will not be discussed. Of the resolved peaks B-J and U-Z, the largest effects are seen for peaks C, E, I, and U-X. The main body of peaks consists of several overlapping resonances that cannot be resolved; however, these also show a general upfield shift. The major peak is initially at −0.25 ppm but shifts to −0.81 ppm. The shifts are gradual throughout the concentration range except for peak D, which only shifts below 2 mM magnesium, i.e., 6 equiv. Peaks E and I only commence shifting after peak D, showing that they are from phosphates with weaker binding constants than D.

As each magnesium effect in the ^{1}H NMR spectra is very local and as the effects occur at several places in the molecule, they cannot be correlated readily with the effects on the scattered peaks in the ^{31}P spectra, which in general are from phosphate groups far from these protons. The magnesium to tRNA ratios for most of the effects in the two types of spectra are also different, which suggests that they are due to different magnesium binding sites. The upfield shifts of the main cluster of peaks in the ^{31}P spectra with increasing magnesium suggest a change in the helical torsion angle of the stems toward a *gg* conformation. This apparently causes little change in the base overlaps as there are only minor changes in the ^{1}H NMR spectra at high magnesium concentrations.

Effect of Temperature. The effect of temperature on the ^{1}H NMR spectrum of tRNA^{Phe} was determined at several magnesium concentrations. As the temperature increases, the imino proton peaks decrease in intensity with little change in shift or line width (spectroscopic melting). This suggests that there is slow exchange from a closed form to a more exposed one followed by fast exchange of protons between the open form and the solvent (Johnston & Redfield, 1977). The temperature at which most of the imino proton peaks melt gradually increases as magnesium is added. The effect of temperature on the proton spectrum at 5 mM magnesium is shown in Figure 5. Most of the peaks shift slightly upfield before melting. While this may be due to some exchange with solvent, peak EE′ moves upfield although it is one of the last protons to melt, and peaks F and L shift downfield with temperature. A downfield shift in an imino proton cannot be due to exchange with solvent and must be due to structural changes on heating. These structural changes are also shown in the ^{31}P NMR spectra discussed below. The downfield shift of peak F with increasing temperature is in the same direction as the

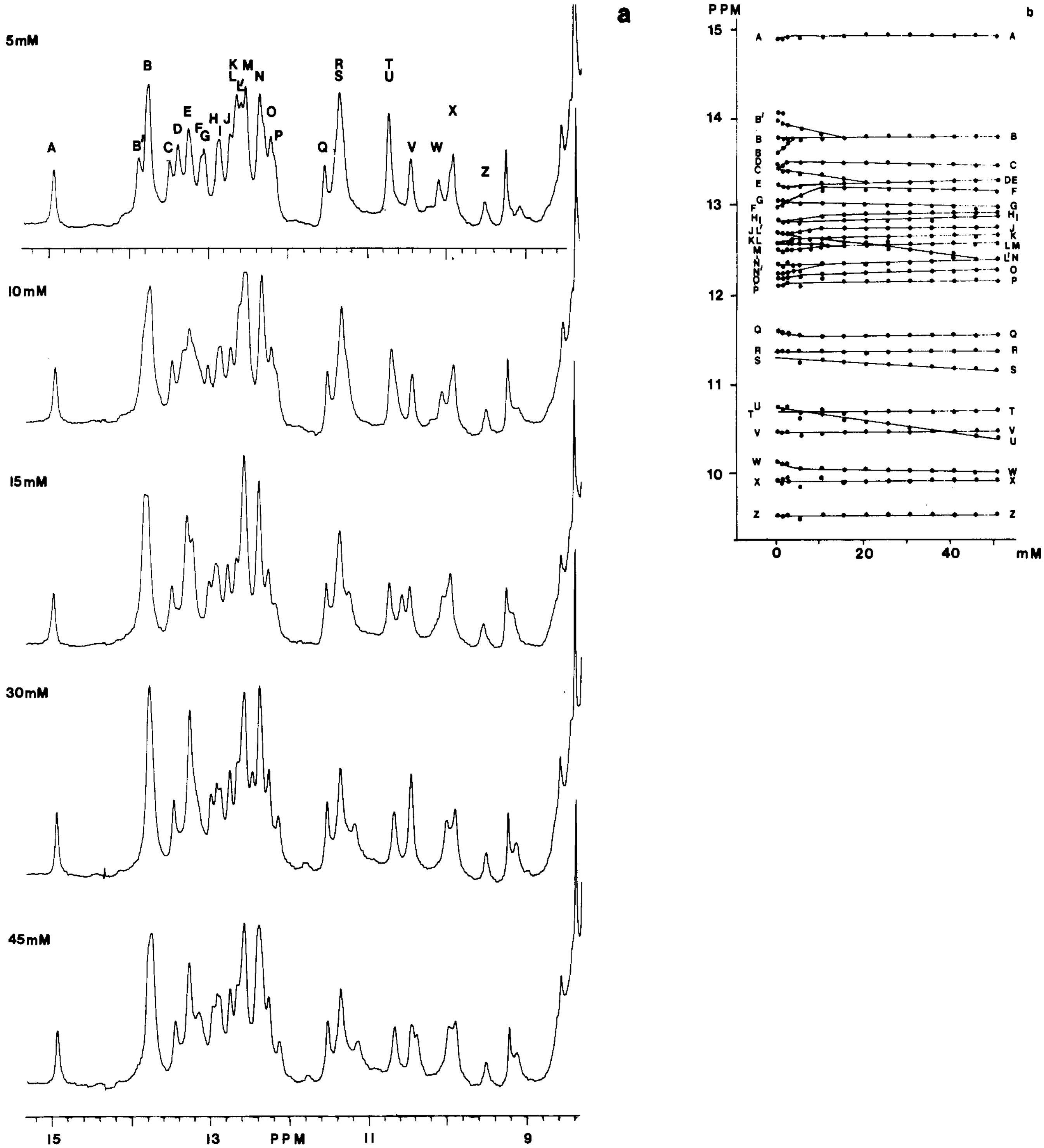

FIGURE 3: Effect of magnesium concentration on the low-field ^{1}H NMR spectra of 1 mM *E. coli* tRNA^{Phe} in 10 mM cacodylate–100 mM NaCl buffer, pH 7.0, at 17 °C. (a) From top to bottom, spectra taken at 5, 10, 15, 30, and 45 mM magnesium. (b) Graph of chemical shifts of peaks vs. magnesium concentration.

shift seen with increasing magnesium. Therefore, the temperature effects do not necessarily reverse the magnesium effects, and magnesium must cause structural changes different from those of temperature. This is also shown in the ^{31}P NMR spectra. Peaks D and P, assigned to the imino protons of AΨ-31 and the tertiary base pair G-15–C-48, respectively, are the most labile in the spectrum followed by peak F, the m^{7}G-46–G-22 tertiary imino proton. Most of the peaks in the D and T stem melt simultaneously at 42 °C. At 57 °C, only six peaks are left, from the acceptor and anticodon stems of the molecule. At low magnesium concentrations and high temperatures a peak at 12.4 ppm is seen that is not observed at higher magnesium concentrations and may be related to the alternate conformations seen in the D stem at low magnesium. Otherwise, the melting behavior at higher magnesium concentrations follows the same pattern as that at 5 mM magnesium (see Figure 9 of the preceding paper).

The thermal unfolding of *E. coli* tRNA^{Phe} observed here is consistent with studies on other tRNA species using temperature jump and calorimetric methods (Crothers & Cole, 1978). From these studies it was concluded that the tertiary structure of tRNA unfolds first followed by the helical stems in order of stability determined by base composition and sequence. In *E. coli* tRNA^{Phe} the acceptor and anticodon stems

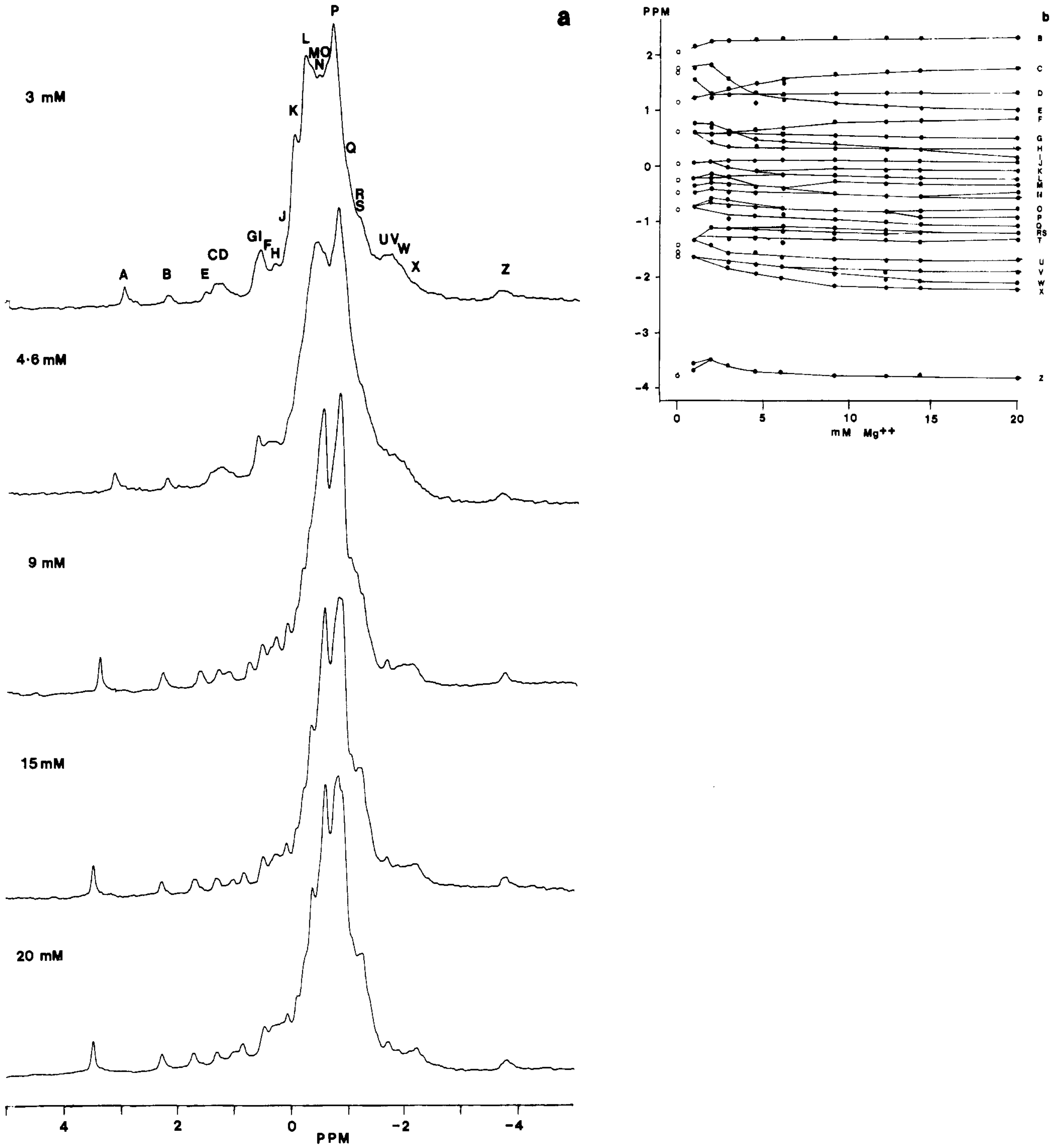

FIGURE 4: Effect of magnesium concentration on the ^{31}P NMR spectra of 0.34 mM *E. coli* tRNA^{Phe} in 10 mM cacodylate–100 mM NaCl buffer, pH 7.0, at 27 °C. (a) From top to bottom, spectra taken at 3, 4.6, 9, 15, and 20 mM magnesium. (b) Graph of chemical shift of phosphate peaks vs. magnesium concentration at 27 °C. (Open circles) Points measured at 7 °C because of melting at 27 °C.

are particularly stable as they contain six and four consecutive GC base pairs, respectively.

In the ^{31}P spectra at 20 mM magnesium, shown in Figure 6, the main peak from the helical stems shows a downfield shift with temperature, suggesting a change in the helical torsion angles. Peaks C and F move upfield, and E moves downfield with increasing temperature, which is opposite to their behavior on increasing the magnesium concentration. However, peaks V and W cross, and peak Z moves downfield. These three effects are not the reverse of the magnesium effects, again suggesting that the structural changes seen with increasing temperature are not all the same as on decreasing the magnesium concentration. Under these conditions there is little differential melting of the scattered peaks. At 67 °C most of the scattered peaks in the ^{31}P spectra shift into the main peaks, leaving only six resolved peaks, namely, A, I, J, K, C or F, and H or F. The ambiguities arise from peaks merging with temperature. In the ^{1}H NMR spectra, the peaks remaining at high temperature are from the acceptor and anticodon part of the molecule. The remaining phosphorus peaks are therefore likely to be from the anticodon loop and the acceptor stem. The phosphates in the anticodon loop and phosphate-76 of the acceptor stem were found to have strained torsion angles in the yeast tRNA^{Phe} crystal structure (Holbrook

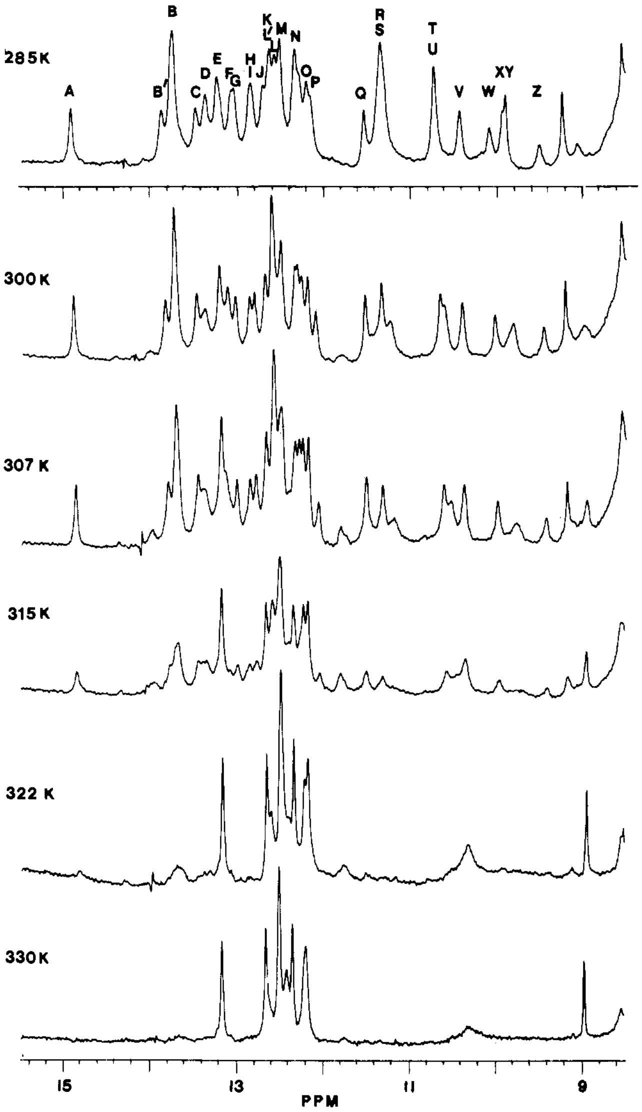

FIGURE 5: Effect of temperature on the low-field ^1H NMR spectra of *E. coli* tRNA^{Phe} in 10 mM cacodylate–100 mM NaCl buffer, pH 7.0, containing 5 equiv of magnesium. From top to bottom, spectra taken at 12, 27, 34, 42, 47, and 57 °C.

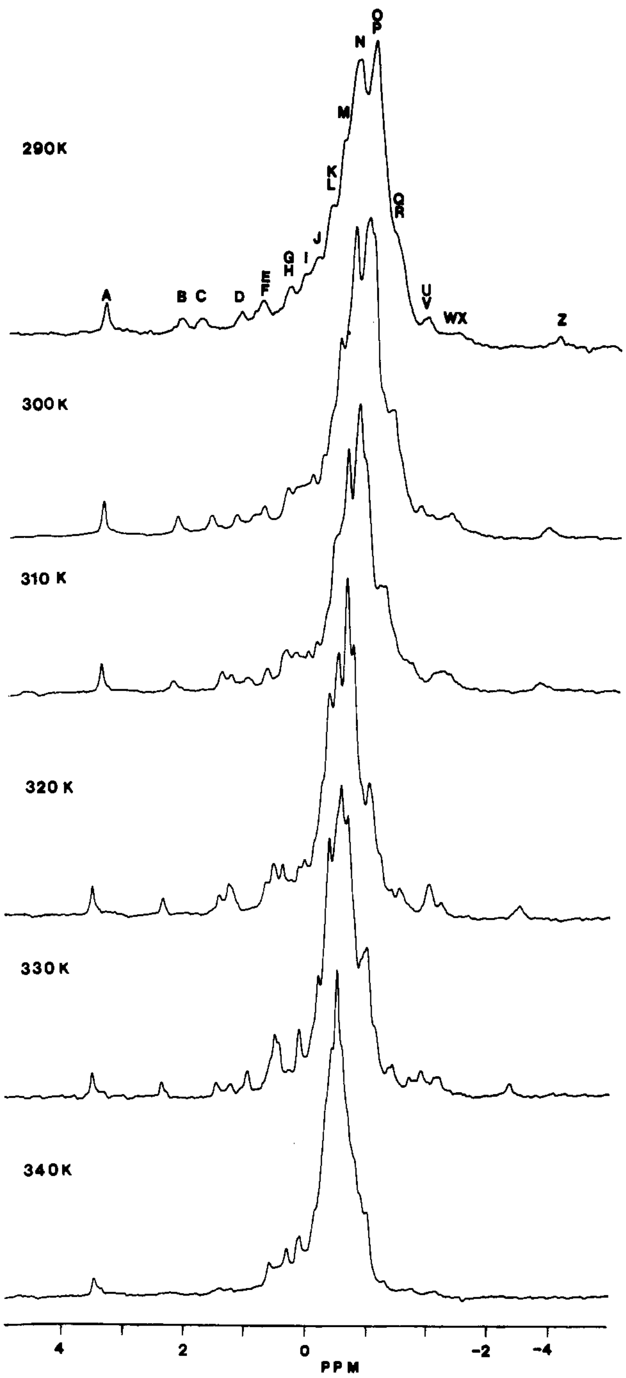

FIGURE 6: Effect of temperature on the ^{31}P NMR spectra of 0.34 mM *E. coli* tRNA^{Phe} in 10 mM cacodylate–100 mM NaCl buffer, pH 7.0, containing 20 mM magnesium. From top to bottom, spectra taken at 17, 27, 37, 47, 57, and 67 °C.

et al., 1978; Jack et al., 1976) and so probably give resolved ^{31}P NMR signals. In the ^{31}P NMR spectrum of yeast tRNA^{Phe}, peaks J and K are not resolved from the major peak, and peaks H and I have not been previously assigned. Peak F was tentatively assigned to the P-10 loop by Gorenstein et al. but to the anticodon loop by Salemink et al. (Gorenstein et al., 1981; Salemink et al., 1981). Recently, Gorenstein et al. have revised their assignment to concur with Salemink et al. (Goldfield et al., 1983). Peak C has been assigned to the anticodon loop by both groups. The assignment of F and C to the anticodon loop suggests that the resolved peaks remaining at high temperature are A, C, F, I, J, and K. From this study, peaks I–K also come from phosphates in the anticodon loop or from P-76.

Effects of Spermine. The effect of spermine on the ^1H NMR spectra was studied at 5 mM magnesium where the resonances are initially best resolved, Figure 7, and at 50 mM magnesium corresponding to the tRNA to magnesium ratio used in the ^{31}P study. All the resonances gradually broaden as spermine is added, partly because of aggregation [at low salt nucleic acids precipitate in the presence of spermine (Hoopes & McClure, 1981)] and partly because spermine, being an amine, catalyzes the exchange of imino and amino protons with solvent. This latter effect is greatest on peaks V and X, which are probably non-hydrogen-bonded imino protons. At 5 mM magnesium, the largest effects of spermine are on resonances D (AΨ-31) and F (m^{7}G-46-C-22), which both merge with EE′, as they do with increasing magnesium. Large shifts are also seen for peaks A and P, which are unaffected by magnesium. These peaks are the resonances of the tertiary imino bonds s^{4}U-8–A-14 and G-15–C-48 at the extension of the D stem. Smaller shift changes are found for peaks G and C, from the neighboring base pairs CG-13 and CG-49. Peak U (Ψ-55 N1-H) shifts downfield, opposite to the effect of magnesium. The other peaks that are affected by magnesium, B$_4$, B′, L′, S, and N′, do not show large effects with spermine. (The effect of spermine on B$_4$ cannot be seen

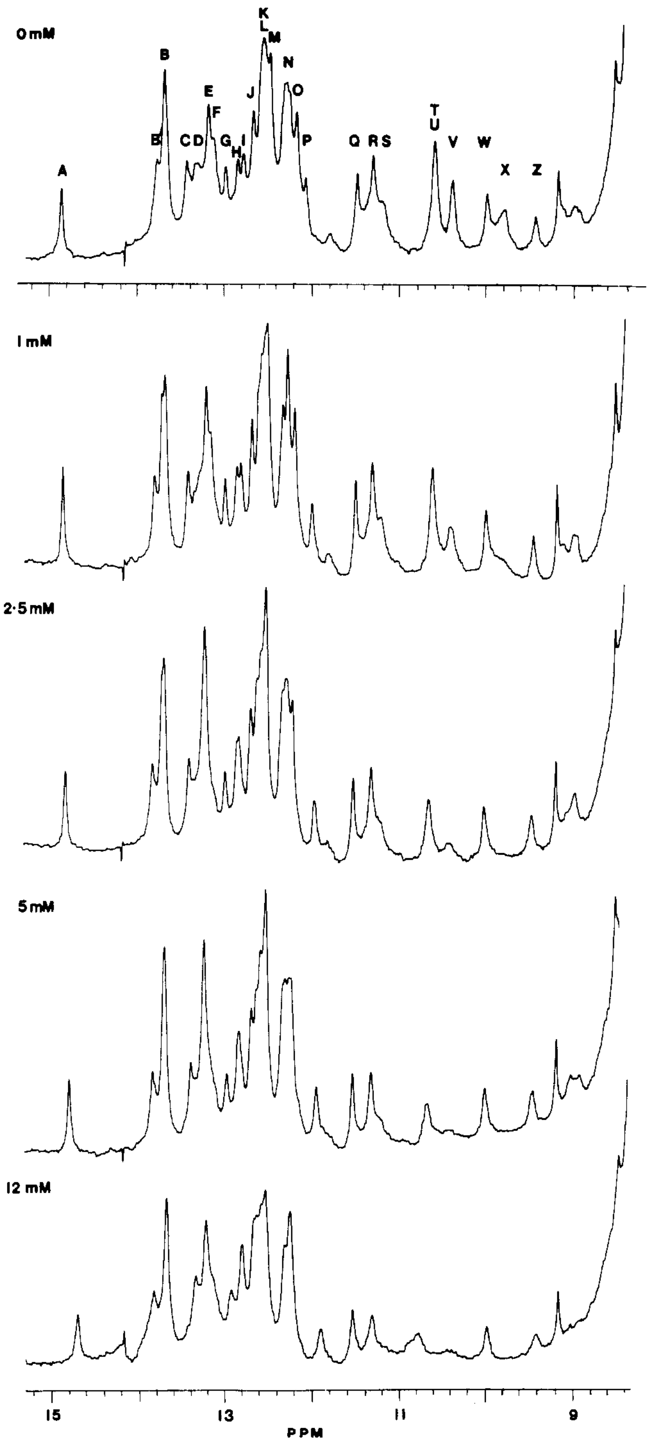

FIGURE 7: Effect of spermine on the low-field ^{1}H NMR spectra of 1 mM *E. coli* tRNA^{Phe} in 10 mM cacodylate–100 mM NaCl buffer, pH 7.0, containing 6 mM magnesium at 27 °C. From top to bottom, spectra taken at 0, 1, 2.5, 5, and 12 mM spermine.

at this magnesium concentration as it has merged with B; however, at high NaCl concentrations, where B$_4$ is separate from B, spermine does not affect its shift.) Thus, the effects on peaks A, P, G, and C are spermine specific while those on B′, L′, S, and B$_4$ are magnesium specific and those on peaks D and F are nonspecific ion effects. At 50 mM magnesium peaks D and F have already merged with EE′; otherwise, the same shift effects with spermine are seen as at 5 mM magnesium.

The specific effects of spermine on the ^{1}H NMR spectrum of tRNA^{Phe} from *E. coli* occur mainly at base pairs G-15–C-48 and s^{4}U-8–A-14. In contrast to the effects of magnesium, the effects of spermine on the ^{1}H NMR spectra occur over several base pairs in a single area of the molecule. This may be because spermine is a long polycation that must bind over several nucleotides in contrast to the smaller, spherical, magnesium ion, which gives more localized effects.

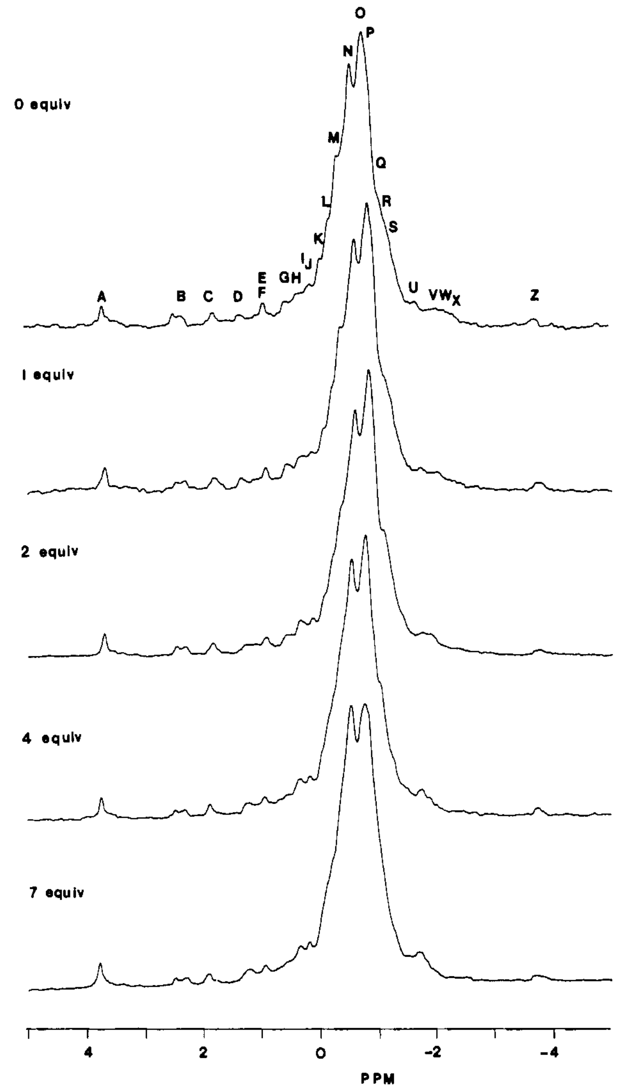

FIGURE 8: Effect of spermine on the ^{31}P NMR spectra of 0.34 mM *E. coli* tRNA^{Phe} in 10 mM cacodylate–100 mM NaCl buffer, pH 7.0, containing 20 mM magnesium at 22 °C. From top to bottom, ^{31}P NMR spectra taken at 0, 1, 2, 4, and 7 equiv of spermine.

For the ^{31}P spectra, the spermine titration was performed at 22 °C and 20 mM magnesium to optimize resolution and is shown in Figure 8. The major effects are on peaks V–X, which move downfield with spermine, in contrast to the effect of magnesium. Peak C shifts downfield, as it does with increasing magnesium, and peak D shifts upfield slightly. The spermine effects in the ^{31}P spectra occur over a similar range of spermine concentrations to those in the proton spectra. Because of this, and also because the effects in the proton spectra occur mainly in one region of the molecule, the effects in the two types of spectra can be correlated. Therefore, peaks D and V–X in the ^{31}P spectra are tentatively assigned as being close to the base pairs G-15–C-48 and s^{4}U-8–A-14, either in the P-10 loop or the variable loop of the molecule. The assignment of peak D to the P-10 loop is consistent with its tight magnesium binding. In the ^{1}H NMR spectrum, tight magnesium binding is observed at peak B$_4$, AU-12. It is also consistent with ^{31}P NMR studies of manganese binding to yeast tRNA^{Phe} in which broadening of peaks A, D, and E and

Table I: Yeast tRNA^{Phe} Ion Binding Sites from X-ray Crystal Structures (Holbrook et al., 1977; Quigley et al., 1978)

ion	direct coordination to	hydrogen bonded to
magnesium		
site 1	phosphate of G-19	phosphate G-19, bases G-20, U-59, C-60, bases G-20, U-59, C-56
site 2	phosphate of G-20, A-21	
site 3		phosphates U-8, A-9, C-11, U-12
site 4	phosphate of Y-37	bases C-32, Y-37, A-38, U-39
spermine		
site 1		phosphates-23, -24, -25, -42, -44
site 2		phosphates-10, -46, -47, -45
site 3	wide grooves of acceptor and T stem	

a high-field peak was observed (Gorenstein et al., 1981). ^{1}H NMR studies show that initial binding of manganese is near the 8–14 and 15–48 tertiary bonds (Hurd et al., 1979). The effect on peak C in the ^{31}P spectra occurs with both magnesium and spermine and is probably a nonspecific ion effect as is that on peak D in the ^{1}H NMR spectra. This is consistent with the assignment of peak C as a phosphate close to AΨ-31, i.e., in the anticodon loop as assigned in yeast tRNA^{Phe}. In the yeast tRNA^{Phe} ^{31}P NMR spectra, peak V (corresponding to peak P in Gorenstein's nomenclature) was initially assigned to the D loop by Gorenstein et al. on the basis of its shift with magnesium, and peaks D and U–X were unassigned (Gorenstein et al., 1981). More recent studies on ethidium bromide binding to yeast tRNA^{Phe} suggest that peaks V–X are near the ethidium bromide site at the P-10 loop (Goldfield et al., 1983) in agreement with the present study.

Comparison with Yeast tRNA^{Phe}. The most studied tRNA species is probably yeast tRNA^{Phe}, which has been independently studied by four groups using X-ray crystallography. The positions and contacts of the magnesium and spermine ions seen in the various crystal structures are given in Table I. The few sites that have been identified are probably the ones with the smallest temperature factors and highest occupancy and so probably correspond to the tightest binding sites.

The ^{31}P spectra of yeast tRNA^{Phe} and *E. coli* tRNA^{Phe} are similar. (Two more peaks are resolved from the major peak at low field in *E. coli* tRNA^{Phe} and one more peak is seen at high field in yeast tRNA^{Phe} ^{31}P NMR spectra.) This suggests that the torsion angles of most of the loop phosphates and, hence, the tertiary structures of the two tRNAs are similar. This is also shown by the NOEs in the ^{1}H NMR spectrum of *E. coli* tRNA^{Phe} in which the same tertiary hydrogen bonds are seen as in the yeast tRNA^{Phe} crystal structure. One difference may be in the anticodon loop of the tRNAs. In *E. coli* tRNA^{Phe}, evidence for an Ψ-32–A-38 base pair was obtained by NOES (preceding paper). Such base pairing is not possible for yeast tRNA^{Phe}. The extra high-field peak in the ^{31}P NMR spectrum of yeast tRNA^{Phe}, not seen in *E. coli* tRNA^{Phe}, may be the one assigned to the anticodon loop. The effects of magnesium and of heating on the ^{31}P spectra of yeast tRNA^{Phe} (Gorenstein & Luxon, 1979; Gorenstein et al., 1981; Salemink et al., 1981) are similar to those seen in *E. coli* tRNA^{Phe}; although the effect of temperature was studied at a different magnesium to tRNA ratio, and the magnesium study was more limited. However, for sperimine binding, Gorenstein & Goldfield found little effect on the ^{31}P spectra of yeast tRNA^{Phe}, except for one peak at high field that shows line broadening (Gorenstein & Goldfield, 1982). This peak is probably absent in *E. coli* tRNA^{Phe} spectra. Thus, magnesium binding to both tRNAs is probably similar while the spermine binding sites may differ.

Unfortunately, the ^{31}P NMR spectrum has not been firmly assigned, and thus one cannot compare the ion effects in solutions with those found in the crystal structure by using ^{31}P NMR. Indeed, conversely, Gorenstein et al. have used the magnesium sites found in the crystal structure to assign the ^{31}P peaks in yeast tRNA^{Phe} that shift with magnesium (Gorenstein et al., 1981). These peaks shift over a wide magnesium concentration range, and thus the changes may not correspond to the magnesium sites found in the crystal structure. The ^{1}H NMR data of *E. coli* tRNA^{Phe} discussed above show a strong magnesium site at base pair 12, which could be related to the magnesium site in the P-10 loop; however, there is little effect at the tertiary base pair s^{4}U-8–A-14, which is thought to be bonded to this magnesium ion also. The shifts seen in peak D, AΨ-31, may correspond to the magnesium site seen in the anticodon loop, but the effects are not ion specific. The two magnesium sites in the D loop at bases 19–21 are not detectable by ^{1}H NMR. The effects on peaks W and H near base pair 52 may correlate with a weakly bound magnesium ion found in the crystal structure of Quigley et al. (1978). The effects of spermine on the ^{1}H NMR spectra suggest that it binds at the junction of the perpendicular helices formed by the T stem and D stem. This may be related to the spermine site at the variable loop found by Quigley et al. (1978).

Conformational changes of tRNA on ion binding characterized in this study have also been postulated for yeast tRNA^{Phe}. In the high-field ^{1}H NMR spectra of the latter, several resonances for the methyl protons of T-54 were observed at intermediate temperatures, suggesting different conformers (Kan et al., 1977; Davanloo et al., 1979). In the ^{31}P NMR studies, Salemink et al. found partial intensity of one peak from a phosphate in the anticodon loop, suggesting that it was in slow exchange with a second, nonresolved peak (Salemink et al., 1981), whereas Gorenstein et al. observed increases in line widths of several peaks at intermediate temperatures, indicating a faster conformational change with an exchange rate of about 30 s^{-1} at 30 °C, 10 mM magnesium (Gorenstein et al., 1981). Temperature-jump studies of yeast tRNA^{Phe} conformation using the fluorescence of the Wye base (Urbanke & Maas, 1978; Ehrlich et al., 1980; Labuda & Porchke, 1980) or of ethidium bromide substituted bases (Ehrenberg et al., 1980; Nilsson et al., 1982) have also demonstrated at least two conformers of the anticondon loop and three in the D loop; however, the exchange rates measured in the different studies varied. Labuda & Porschke measured an exchange rate of 800 s^{-1} between two conformers while Ehrenberg et al. measured two slower exchange rates between three conformers. In the latter study, $k_{1,2}$ was 95 s^{-1} and $k_{3,2}$ was 14 s^{-1} at 24 °C and zero magnesium, slowing to 15 s^{-1} and 2 s^{-1} at 1 mM magnesium. This last rate is similar to that found in the present study of *E. coli* tRNA^{Phe} at less than 0.1 equiv of magnesium, namely, 1.3 s^{-1} at 17 °C. The proportions of the states T2 and T3 in the Ehrenberg study, 2:1 at high magnesium, is also close to the 3:1 ratio found at low magnesium in this study. This NMR study was performed at a tRNA concentration of 1 mM whereas the fluorescence studies were performed at a tRNA concentration of 1 μM. The latter is below the dissociation constant of the most tightly binding magnesium ion, estimated to be about 10^{-4} M (Schreier & Schimmel, 1974; Ehrenberg et al., 1979); therefore, the number of bound magnesium ions at 10 mM magnesium in the fluorescence study may be the same as the 0.1 equiv of magnesium in the present study. Thus, the slow change in the

Table II: ^{31}P NMR Assignments

E. coli tRNA^{Phe}		yeast tRNA^{Phe}			
		Gorenstein and Goldfield[a]		Salemink[b]	
peak	assignment	peak	assignment	peak	assignment
A	5′ P	A	5′ P	a	5′ P
B		B		b	
C	anticodon	C	Y-37	c	anticodon
D	P-10 loop	D		d_1	P-10 loop or variable loop
E		E	P-10 loop	d_2	P-10 loop or variable loop
F	anticodon	F	anticodon	e	anticodon
G		F′, G			
H		H			
I	anticodon or P-76	I			
J	anticodon or P-76				
K	anticodon or P-76				
L					
M		J			
N		K			
O		L			
P		M			
Q		N			
R		O	P-10 loop	g	P-10 loop or variable loop
S					
T		Q		h_1	P-10 loop or variable loop
U					
V	P-10 loop or variable loop	P	D loop	h_2	
W	P-10 loop or variable loop	R	P-10 loop	i_1	
X	P-10 loop or variable loop	S		i_2	D loop or T loop
Z		T	D loop	j_1	D loop or T loop
		U	U-33	j_2	P-36

[a] Gorenstein et al., 1981; Goldfield et al., 1983. [b] Salemink et al., 1979, 1981.

D stem observed in this study of *E. coli* tRNA^{Phe} may be related to the T2 to T3 conformational transition observed in both the D loop and anticodon loop in yeast tRNA^{Phe}. The T3 conformation was shown to be favored by both magnesium and spermine (Ehrenberg et al., 1979; Nilsson et al., 1982).

SUMMARY AND CONCLUSIONS

We have characterized several changes in *E. coli* tRNA^{Phe} on addition of ions. At low ion concentrations *E. coli* tRNA^{Phe} exists as a mixture of two conformations in slow exchange, differing at base pairs 12 and 13 in the D stem. The proportion of each is ion dependent but not ion specific. At higher magnesium ion concentrations only fast exchange between resonances was observed in the present study despite some large chemical shift changes, suggesting much faster conformational changes. The hydrogen-bonded imino protons of AΨ-31 and m^{7}G-46 bind ions nonspecifically and are relatively labile with respect to temperature, suggesting that their conformations are easily altered. Magnesium affects protons in all the helical stems with the tightest binding site observed perturbing AU-12; however, each effect is local. In contrast, spermine affects several protons near s^{4}U-8–A-14 and G-15–C-48. Ion binding causes some structural changes different from those caused by temperature. Correlation of the ion effects observed in the ^{1}H and ^{31}P NMR spectra and the resolved peaks stable at high temperature in both spectra has led to tentative assignments of some of the ^{31}P NMR resonances. These are summarized in Table II together with the assignments of the corresponding peaks in yeast tRNA^{Phe} (Gorenstein et al., 1981; Salemink et al., 1981).

Although the ion effects observed in these spectra occur near the in vivo concentration of the ions, too little is known at present about the interactions of tRNA with proteins and ribosomes to know which effects and which tRNA conformations are biologically relevant. Some aminoacyl-tRNA synthetases have been shown to interact with the U-8 base of tRNAs (Schoemaker & Schimmel, 1977), and some also recognize the anticodon (Bruce & Uhlenbeck, 1982). This suggests that the changes observed in the D stem may be of importance in aminoacylation while the flexibility of AΨ-31 may be of importance both in aminoacylation and in codon–anticodon binding.

ACKNOWLEDGMENTS

We are grateful to Susan Ribeiro for purification of the *E. coli* tRNA^{Phe} and to Gary Drobny for assistance with the NMR instruments.

SUPPLEMENTARY MATERIAL AVAILABLE

Three figures showing a saturation–recovery experiment on peak G at low magnesium concentrations (spectra at different times after irradiation and graph of results), a graph of ^{31}P chemical shifts vs. temperature, and a graph of ^{1}H chemical shifts vs. spermine concentration (4 pages). Ordering information is given on any current masthead page.

Registry No. Mg, 7439-95-4; spermine, 71-44-3.

REFERENCES

Arter, D. M., & Schmidt, P. G. (1976) *Nucleic Acids Res. 3*, 1437.

Bruce, A. G., & Uhlenbeck, O. C. (1982) *Biochemistry 21*, 3921.

Crothers, D. M., & Cole, P. E. (1978) in *Transfer RNA* (Altman, S., Ed.) p 196, MIT Press, Cambridge, MA.

Davanloo, P., Sprinzl, M., & Cramer, F. (1979) *Biochemistry 18*, 3189.

Ehrenberg, M., Rigler, R., & Wintermeyer, W. (1979) *Biochemistry 18*, 4588.

Ehrlich, R., Lefevre, J. F., & Remy, P. (1980) *Eur. J. Biochem. 103*, 145.

Forsen, S., & Hoffman, R. A. (1963) *J. Chem. Phys. 39*, 2892.

Gillam, I., Millward, S., Blew, D., Van Tigerstrom, M., Wimmer, E., & Tener, G. N. (1967) *Biochemistry 6*, 3043.

Goldfield, E. M., Luxon, B. A., Bowre, V., & Gorenstein, D. G. (1983) *Biochemistry 22*, 3336.

Gorenstein, D. G. (1975) *J. Am. Chem. Soc. 97*, 898.

Gorenstein, D. G., & Kar, D. (1975) *Biochem. Biophys. Res. Commun. 65*, 1073.

Gorenstein, D. G., & Kar, D. (1977) *J. Am. Chem. Soc. 97*, 672.

Gorenstein, D. G., & Luxon, B. A. (1979) *Biochemistry 18*, 3796.

Gorenstein, D. G., & Goldfield, E. M. (1982) *Biochemistry 21*, 5839.

Gorenstein, D. G., Goldfield, E. M., Chen, R., Kovar, K., & Luxon, B. A. (1981) *Biochemistry 20*, 2141.

Gueron, M., & Shulman, R. G. (1975) *Proc. Natl. Acad. Sci. U.S.A. 72*, 3482.

Hingerty, B., Brown, R. S., & Jack, A. (1978) *J. Mol. Biol. 124*, 523.

Holbrook, S. R., Susman, J. L., Warrant, R. W., Church, G. M., & Kim, S.-H. (1977) *Nucleic Acids Res. 4*, 2811.

Holbrook, S. R., Sussman, J. L., Warrant, R. W., & Kim, S.-H. (1978) *J. Mol. Biol. 123*, 631.

Biochemistry **1985**, *24*, 4325–4332 4325

Hoopes, B. C., & McClure, N. R. (1981) *Nucleic Acids Res. 9*, 5493.

Hurd, R. E., Azhderian, E., & Reid, B. R. (1979) *Biochemistry 18*, 4012.

Hyde, E. I., & Reid, B. R. (1985) *Biochemistry* (second paper of three in this issue).

Jack, A., Ladner, J. E., & Klug, A. (1976) *J. Mol. Biol. 108*, 619.

Jack, A., Ladner, J. E., Rhodes, D., Brown, R. S., & Klug, A. (1977) *J. Mol. Biol. 111*, 315.

Johnston, P. D., & Redfield, A. G. (1977) *Nucleic Acids Res. 4*, 3599.

Kan, L. S., Ts'o, P. O. P., Sprinzl, M., v.d. Haar, F., & Cramer, F. (1977) *Biochemistry 16*, 3143.

Labuda, D., & Porchke, D. (1980) *Biochemistry 19*, 3799.

Loftfield, R. B., Eigner, E. A., & Pastuszyn, A. (1981) *J. Biol. Chem. 256*, 6729.

Lovgren, T. N. E., Petersson, A., & Loftfield, R. B. (1978) *J. Biol. Chem. 256*, 6702.

Nilsson, L., Rigler, R., & Wintermeyer, W. (1982) *Biochim. Biophys. Acta 740*, 460.

Nishimura, S. (1971) in *Procedures in Nucleic Acid Research* (Cantoni, G. L., & Davies, D. R., Eds.) Vol. 2, p 542, Harper and Row, New York.

Noggle, J. H., & Shirmer, R. E. (1971) *The Nuclear Overhauser Effect: Chemical Applications*, Academic Press, New York.

Quigley, G. J., Teeter, M. M., & Rich, A. (1978) *Proc. Natl. Acad. Sci. U.S.A. 75*, 64.

Reid, B. R. (1981) *Annu. Rev. Biochem. 50*, 969.

Salemink, P. J. M., Swarthof, T., & Hilbers, C. W. (1979) *Biochemistry 18*, 3477.

Salemink, P. J. M., Reijerse, E. J., Mollevanger, L., & Hilbers, C. W. (1981) *Eur. J. Biochem. 115*, 635.

Sanchez, V., Redfield, A. G., Johnston, P. D., & Tropp, J. (1980) *Proc. Natl. Acad. Sci. U.S.A. 77*, 5659.

Schimmel, P. R., & Redfield, A. G. (1980) *Annu. Rev. Biophys. Bioeng. 9*, 181.

Schoemaker, H. J. P., & Schimmel, P. R. (1977) *Biochemistry 16*, 5454.

Schreier, A. A., & Schimmel, P. R. (1974) *J. Mol. Biol. 86*, 601.

Schreier, A. A., & Schimmel, P. R. (1975) *J. Mol. Biol. 93*, 323.

Stein, A., & Crothers, D. M. (1976a) *Biochemistry 15*, 157.

Stein, A., & Crothers, D. M. (1976b) *Biochemistry 15*, 160.

Thompson, R. C., Dix, D. B., Gerson, R. B., & Karim, A. M. (1981) *J. Biol. Chem. 256*, 6676.

Urbanke, C., & Maas, G. (1978) *Nucleic Acids Res. 5*, 1551.

Conformations of Two Duplex Forms of d(TCGA) in Slow-Exchange Equilibrium Characterized by NMR[†]

David G. Reid, Stephen A. Salisbury, Tom Brown, and Dudley H. Williams*

University Chemical Laboratory, Cambridge, CB2 1EW U.K.

Received October 11, 1984; Revised Manuscript Received March 6, 1985

ABSTRACT: Two conformations adopted by the tetranucleoside triphosphate d(TCGA) in aqueous solution are in slow-exchange equilibrium on the NMR time scale. ^{1}H and ^{31}P NMR spectra obtained at temperatures below 25 °C contain two sets of signals that vary in relative proportions with changing temperature. High-field NMR techniques allow the conformations of these species to be examined. Both forms are right-handed double-helical structures, and their interconversion does not involve a single-stranded species since transfer of saturation is observed between corresponding imino protons held in the base pairs of each duplex. The form that predominates at higher temperatures resembles B-DNA, but the other, while of similar conformation at the ends of the molecule, is distorted at the C-G step. Shearing at the center of the duplex results in interstrand stacking of the two cytosines in a way that is reminiscent of Z-DNA. Distances between nonexchangeable protons in this model are consistent with nuclear Overhauser effects observed for resonances of the low-temperature form, while the ^{1}H NMR spectrum shows cytidine H-2′ resonances at unusually high field. The relative stabilities of the two forms are discussed in terms of base stacking and hydration, but the origin of the high activation energy for interconversion implicit in the slow-exchange rate is unclear. The conformation of the low-temperature form may represent a sequence-dependent structural feature important in natural DNA, although somewhat fortuitously exemplified by this tetramer. The suggested involvement in correct nucleosome phasing of the pentamer d(TTCGA), present in some eukaryotic genes, is noted.

The double-helical structures formed by nucleic acids are classically built up as a succession of interchangeable nucleotide pairs. Despite the potential of this arrangement for regularity, high-resolution, single crystal X-ray analysis of oligonucleotide fragments of A- and B-DNA (Drew et al., 1980; Viswamitra et al., 1978; Conner et al., 1982; Wang et al., 1982; Shakked et al., 1983) have shown considerable variation from the classical geometries derived by using data from polymeric DNA. In B-type structures, this variation has been correlated with the properties of polynucleotides in solution (Klug et al., 1979; Lomonossoff et al., 1981) and is

---

[†] This work was supported by the Medical and Science and Engineering Research Councils, United Kingdom.

0006-2960/85/0424-4325$01.50/0